High-resolution spectroscopy and high-density monitoring in X-rays of novae[*]

J. U. Ness[†]

XMM-Newton Science Operations Centre, ESA, PO Box 78, 28691 Villanueva de la Cañada, Madrid, Spain

Abstract. The 21st century X-ray observatories *XMM-Newton, Chandra,* and *Swift* gave us completely new insights into the X-ray behaviour of nova outbursts. These new-generation X-ray observatories provide particularly high spectral resolution and high density in monitoring campaigns, simultaneously in X-rays and UV/optical. The entire evolution of several nova outbursts has been observed with the *Swift* XRT and UVOT instruments, allowing studies of the gradual shift of the peak of the SED from UV to X-rays, time scales to the onset and duration of the X-ray brightest supersoft source (SSS) phase, and pre- and post-SSS X-ray emission. In addition, *XMM-Newton* and *Chandra* observations can efficiently be scheduled, allowing deeper studies of strategically chosen evolutionary stages. Before *Swift* joined in 2005, *Chandra* and *XMM-Newton* blind shots in search of SSS emission unavoidably led to some under-exposed observations taken before and/or after the SSS phase. More systematic *Swift* studies reduced this number while increasing the number of novae. Pre- and post-SSS spectra at low and high spectral resolution were successfully modelled with collisional plasma models. Pre-SSS emission arises in shocks and post-SSS emission in radiatively cooling thin ejecta. In contrast, the grating spectra taken during the SSS phase are a lot more complex than expected and have not yet been successfully modeled. Available hot white dwarf (WD) radiation transport models give only approximate reproduction of the observations, and make some critical assumptions that are only valid in isolated WDs. More grating spectra would be important to search for systematic trends between SSS spectra and system parameters.

Summary of well-established discoveries with *Swift, XMM-Newton,* and *Chandra:*
• About 50% of novae display faint X-ray emission before the start of the SSS phase
• The start of the SSS phase is not a smooth process. High-amplitude variations during the early SSS phase were seen that disappear close to the time when the optical plateau

---

phase begins.
- The end of the SSS phase is in most cases a smooth process.
- The SSS grating spectra contain continuum spectra that roughly resemble a black-body shape
- The SSS X-ray grating spectra of systems with known high inclination angles contain emission lines on top of the continuum
- The SSS X-ray spectra of systems with unknown or low inclination angles contain deep absorption lines from the interstellar medium and local, high-ionisation absorption lines that are blue shifted.

1.   Introduction

Classical Novae (CNe) occur in cataclysmic binary systems (CVs) in which the close companion star provides H-rich nuclear burning fuel that is transferred to the surface of the white dwarf (WD) primary via accretion. Once enough hydrogen-rich material is accumulated, a thermonuclear runaway triggers the initial explosion. The radiative energy output exceeds the Eddington limit and drives an optically thick wind. The way we observe a nova from Earth depends on the properties of the ejected material. Absorption and scattering change the colour of the light that originates from the central nuclear burning processes. During radiative transport through the optically thick part of the ejecta, the peak of the broad-band spectrum (or spectral energy distribution, SED), is shifted to successively lower energy. Observed optical light arises after radiation transport through a larger column than X-ray emission. The opacity evolution of the ejecta may or may not be a homogeneous process, but the bolometric luminosity should be dictated by the energy budget of central nuclear burning that is believed to be constant until all hydrogen burning material has been consumed or ejected (Gallagher & Starrfield 1976). With the continuously shifting SED, observations of nova evolution require multiwavelength monitoring, including the UV and X-ray bands. The last evolutionary phase before a nova turns off is the supersoft source (SSS) phase, during which atmospheric X-ray emission from the central regions of the ejecta, close to the surface of the WD, can be observed. The start of the SSS phase depends on the opacity evolution of the ejecta and can not be predicted accurately. Before and after the SSS phase, novae are X-ray faint, and scheduling X-ray observations yields a risk of non-detections if observed too early or too late. Recent dense X-ray/UV monitoring observations obtained with the *Swift* satellite give important insights into the long-term opacity evolution of the ejecta, also facilitating more accurate scheduling of deeper X-ray observations, employing the grating spectrometers on board *XMM-Newton* and *Chandra*. X-ray grating spectra yield higher *spectral* resolution, allowing determinations of physical properties such as the energetics of nuclear burning, mass of the underlying WD, and chemical composition. Followup X-ray observations are also of longer con-

tinuous durations, allowing studies of short-term ($10^2 - 10^4$ s) variability and associated spectral changes.

In this review, I summarise observing strategies to catch the SSS phase, at first via educated guesses based on theoretical expectations and observational evidence from optical (Section 4.2), and later assisted with *Swift* monitoring observations (Section 4.3). I only touch on some selected nova observations to exemplify the key points of observing strategies and data analysis. More general conclusions from the entirety of all observations are presented in Section 5.

2. A brief history of past X-ray observations of novae

Before the advent of *Chandra* and *XMM-Newton*, instruments of moderate sensitivity and spectral resolution but large fields of view were available. In surveys of the Large Magellanic Cloud (LMC) with the Einstein Observatory, a few mysterious luminous sources with extremely soft spectra were discovered (Long, Helfand & Grabelsky 1981) which were later combined in a new class of Super Soft Sources (SSS) after more had been discovered with *ROSAT* (Kahabka, Pietsch & Hasinger 1994; Greiner, Hasinger & Kahabka 1991). The underlying systems were identified as accreting WDs with ongoing nuclear burning on their surface (Kahabka & van den Heuvel 1997). Since novae occur in such systems, the concept of constant bolometric luminosity throughout the evolution with a continuous shift of the peak of the SED towards higher energies, predicts that they emit SSS X-ray spectra during their late, X-ray bright, phase (Gallagher & Starrfield 1976). This was confirmed by, e.g., *EXOSAT* and *ROSAT* observations (Ögelman, Krautter & Beuermann 1987). Monitoring observations over time intervals of 2-3 years resulted in rough light curves that could be divided into a rise phase, plateau phase, and decline phase (Krautter et al. 1996).

The available X-ray detectors of the time allowed no precise measurements of photon energies, leaving uncertainties of several 10-100 eV. Nevertheless, the term 'X-ray spectrum' is occasionally used for 30-100 channel distributions of photon energies. Obviously, no detailed spectral modelling is possible with such data, and the first spectral characterisations consisted of mere blackbody fits yielding effective temperatures of several 10 eV (a few 10^5 K) and bolometric luminosities near or even beyond the Eddington limit (for electrons) of a 1-$M_\odot$ WD. Such high values of luminosity, several months to years after the initial outburst, imply an unphysically high total mass loss. In light of the incorrect assumption of a blackbody model (thermal equilibrium), the corresponding best-fit parameters have no physical meaning. In an attempt to derive more physically meaningful results, atmosphere models were applied. For example, Balman, Krautter & Ögelman (1998) determined a lower luminosity from LTE atmosphere model fits. However, including further more physics of non-LTE models, yield different luminosities again, e.g., Hartmann & Heise (1997). When calling in mind the small number of observed energy channels, one may wonder whether atmosphere models with their high degree of complexity are sufficiently constrained by the data. *The dilemma of the low-resolution spectra is that good fits to the data can be achieved with either well-constrained but unphysical models or with more physical but unconstrained models. None of these approaches can lead us to truly informative results.*

Substantially higher spectral resolution is undoubtedly needed, and the *Chandra* and *XMM-Newton* missions with their grating spectrometers (see Section 3.1) are a great leap forward. This article concentrates on the *Swift* and *XMM-Newton/Chandra* light curves and spectra. For more information on early X-ray observations of novae, I refer to reviews by Krautter (2002, 2008); Starrfield, Iliadis & Hix (2008); Bode & Evans (2008).

3.   Current-day X-ray observing facilities

In the following subsections, the instrumentation of *XMM-Newton*, *Chandra*, and *Swift* is described in brevity.

3.1   *XMM-Newton* and *Chandra*

Chandra and *XMM-Newton* carry CCD spectrometers with similar energy resolution of previous missions but with higher sensitivity and spatial resolution. In addition, much higher spectral resolution can be achieved with the new gratings. The dispersed photons are recorded by X-ray sensitive detectors whose spatial resolution determines the spectral resolution of the extracted spectrum. *XMM-Newton* carries three X-ray mirrors with one directing all light on a single pn CCD detector array (Strüder et al. 2001) while the light from the other two mirrors are shared between Metal Oxide Semi-conductor (MOS) detectors (Turner et al. 2001) and Reflection Grating Spectrometers (RGS; den Herder et al. 2001). The wavelength range of RGS1 and RGS2 is 6-38 Å, and the wavelength resolution is ~ 0.06 Å.

The *Chandra* mission carries two grating spectrometers, a Low- and a High- Energy Transmission Grating (LETGS and HETGS), covering the wavelength ranges 1-175 Å and 1-35 Å, with wavelength resolutions of 0.06 and 0.01 Å, respectively. As recording devices, a microchannel high-resolution image (HRI) detector and chip arrays of the Advanced CCD Imaging Spectrometer (ACIS) are available and can be combined depending on scientific demands. The LETGS/HRC-S combination covers a wavelength range from 1-175 Å at 0.06 Å resolution, and the HETGS/ACIS-S combination covers 1-38 Å at 0.02 Å resolution. The LETGS/ACIS-S combination (1-38 Å at 0.06 Å resolution) is sometimes used for higher effective areas at 20-38 Å at the expense of spectral resolution compared to HETGS/ACIS-S and wavelength coverage compared to LETGS/HRC-S. The ACIS detector allows order sorting, thus the removal of higher-dispersion order photons overlapping with first-order photons, taking advantage of the energy resolution of the ACIS. The HRC does not have sufficient energy resolution for order sorting, but suffers no pileup. Order sorting is also possible with the *XMM-Newton/RGS*.

3.2   *Swift* γ/UV/X-ray Observatory

The primary purpose of *Swift* is to detect γ-ray bursts (GRB) and carry out rapid follow up observations in the X-ray and UV bands. The satellite was thus designed with extremely short slew times between distant targets in the sky. The required instrumentation needs to be sensitive from γ rays via X-rays, down to UV and optical. A GRB detected by the Burst Alert Telescope

(BAT) can then be followed up with the X-Ray Telescope (XRT; Burrows et al. 2005) and finally with Ultra-Violet/Optical Telescope (UVOT; Roming et al. 2005). The XRT and UVOT resemble the Metal Oxide Semi-conductor (MOS) and the Optical Monitor (OM) on board *XMM-Newton*, respectively. The XRT allows a more precise determination of the position of a GRB and rough spectral parameters such as flux and neutral hydrogen column density, N_{H}. Deeper observations with more sensitive observatories such as *Chandra* or *XMM-Newton*, but also by Suzaku, can be planned, and adequate exposure times can be calculated.

Owing to its low-Earth orbit of ∼ 96 minutes, *Swift* can take no long, continuous observations. The maximum visibility for the majority of targets is ∼ 2 ks (depending on declination). Deeper *Swift* observations therefore consist of multiple short snapshots. Photometric studies are only possible for variations on time scales of days or on very short time scales of seconds to minutes.

Swift detects about 90 GRBs a year and spends some ∼ 20 − 30% of the available observing time for followups (Kim Page, private communication). More than half of the *Swift* time budget can be filled with observations of other targets. The low-Earth orbit allows only short snapshots of a few hundred seconds every 96 minutes, each yielding an X-ray and UV/optical flux plus some spectral information. While the resulting X-ray spectra can not compete against those obtained from long, uninterrupted *Chandra* or *XMM-Newton* observations, large series of *Swift* snapshots over extended periods of time are of high value to monitor the X-ray and UV evolution of variable sources such as supernovae, novae, and X-ray binaries, in unprecedented detail.

4. X-ray observations of novae

A large number of *Swift, XMM-Newton,* and *Chandra* observations of novae have been taken, not all of which can be discussed in this review. Early *Swift* observations focused on single detections of older novae, while a prolific monitoring program was developed after the initial monitoring of the prestigious recurrent nova RS Oph was extremely successful. Some examples are described in Section 4.1. Before these monitoring observations were done, *XMM-Newton* and *Chandra* had to dig in the mist to catch the important SSS phase with the X-ray gratings, which is described in Section 4.2. The time by which the SSS phase should start, and thus the best time for deep X-ray grating observations, is not well constrained by observations in other wavelength bands. For example, an indicator for the presence of SSS emission could be observations of high-ionisation optical lines (Schwarz et al. 2011). *Swift*-assisted grating observations are much more efficient, which is described in Section 4.3. I touch on individual novae, describing the respective observing strategies and some results from data analysis. Beyond the examples given here, there are a lot more, and for further reading, I recommend Schwarz et al. (2011). I focus on the spectral analysis with only a brief mention of additional timing analysis.

4.1 *Swift* observations

The first *Swift* observations of novae addressed the question whether or not any significant post-outburst emission was still present from previous novae. For example, V1494 Aql (see Sec-

tion 4.2) was observed three times, more than six years after outburst, and was not detected. Meanwhile, V4743 Sgr that was observed four years after outburst, yielded a clear detection. The old nova V723 Cas from 1995 had never been observed in X-rays until *Swift* offered a first observation at lower price than *Chandra* or *XMM-Newton*. The continuous rise of high-ionisation emission lines in optical spectra had suggested the presence of a hot photoionising source which could be directly visible in X-rays (Schwarz et al. 2011). Indeed, a clear SSS spectrum was found, 14 years after outburst (Ness et al. 2008). The further evolution was followed with more *Swift* observations and later also with two *XMM-Newton* observations. V723 Cas is now the record holder with the latest X-ray detection on day 6018, 16.5 years after outburst.

A first summary of X-ray observations with *Swift* in comparison to previous programs is shown in the left panel of Fig. 1, taken from Ness et al. (2007a). At that time, multiple X-ray observations of the same nova were rather the exception than the rule, and the sample included a large range of speed classes for different novae. An updated description of the *Swift* archive of nova observations was presented by Schwarz et al. (2011), focusing on comparisons of the large monitoring programs. In the right panel of Fig. 1, colour codes are used to mark different phases based on spectral shapes and brightness, as described in the caption. The arrangement in vertical direction is an indicator for the speed class, using the full width at half maximum (FWHM) line width of optical lines (values given in right and left). With narrower FWHM (thus slower speed class), the SSS phase occurs later in the evolution.

The long-term *Swift* X-ray (and partly simultaneous UV) light curves are presented, e.g., in Schwarz et al. (2011), eight of these are shown in Fig. 2, where *XMM-Newton* and *Chandra* observations are marked by blue and orange lines, respectively (see below). Each plot has a different y-scale, and to give an impression of the respective brightness levels, the maximum count rates are marked with a horizontal dashed line with values in units counts per second (cps) given in the left. Two orders of magnitude in count rate have been encountered.

The first dense *Swift* X-ray monitoring programme of a nova was carried out following the 6th recorded outburst of the recurrent symbiotic nova RS Oph in February 2006 (Page et al. 2008; Osborne et al. 2011, second panel in left column in Fig. 2). The X-ray brightness evolution was followed until long after the nova had turned off. The early shock phase, the SSS phase, and the decline phases were all extremely well covered with brightness and spectral information. An illustration of the available *Swift* data is shown in the top plot in Fig. 3. The early shock phase can be seen in the spectral brightness map above 1 keV, while the later SSS phase covers the range between 0.3-0.9 keV in energy and 30-90 days after outburst in time. The early shock phase was analysed by Bode et al. (2006), and the evolution of shock velocity was derived, using the plasma temperature that was derived from collisional plasma models to the *Swift* spectra. Later, Vaytet et al. (2011) used hydrodynamic models yielding much higher shock velocities, indicating that the gas temperature from standard models is not the ideal way to assess the shock velocity. In addition to high shock velocities, a rather low ejecta mass was found. The models were only applied to the low-resolution *Swift* spectra, excluding the SSS component in the later observations. While the standard models by Bode et al. (2006) also reproduce the high-resolution grating spectra (Ness et al. 2009b), this has not yet been tested with the hydro model used by Vaytet et al. (2011).
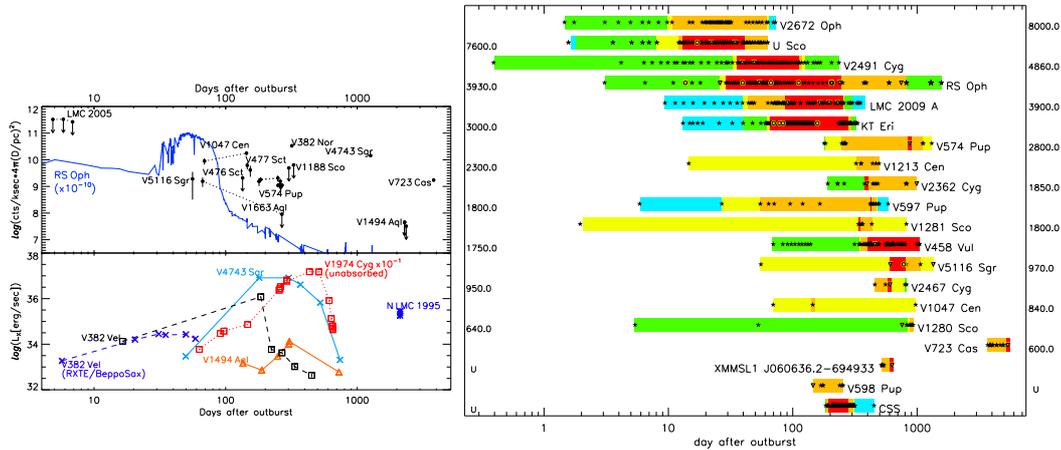
Figure 1. Overview of *Swift* monitoring observations of novae. **Left** from Ness et al. (2007a): X-ray fluxes as function of time after respective outburst. The top panel shows the *Swift* data available in 2007 and the bottom one the same for data from other missions. The RS Oph *Swift* light curve (that was not included in Ness et al. 2007a) is added in purple for comparison. **Right** from Schwarz et al. (2011): Overview of results from *Swift* monitoring campaigns of novae in which SSS emission was observed. The colours are: light blue: non-detections, green: detections but no clear or hard spectrum, yellow: possible SSS emission, orange weak SSS emission, red: strong SSS emission. The plot symbols indicate times when observations were taken with *Swift* (stars), *XMM-Newton* (triangles), and *Chandra* (circles). The novae are arranged by increasing optical emission line FWHM with values shown either left or right of the source. "U" is used for novae with unknown FWHM velocities. For larger versions, see original articles.

The evolution of RS Oph during the rise phase into the SSS phase led to some initial confusion as the nova seemed to turn off quicker than expected but then increased again in flux (Osborne et al. 2006a). Continued monitoring revealed a high-amplitude variability phase during the early SSS phase (Osborne et al. 2006c). RS Oph turned out not to be unique in having an early variability phase as other nova monitoring observations displayed the same. For example, in the slower nova V458 Vul (Ness et al. 2009a), a steep drop in count rate after the initial rise of SSS emission occurred around day 410 (bottom right of Fig. 2). The on- and off states during the early SSS phase were in fact strictly anticorrelated to the UV (Schwarz et al. 2011). The same phenomenon was seen in several other novae (see Fig. 2 and Schwarz et al. 2011), allowing the conclusion that **high-amplitude variations are a common phenomenon during the early SSS phase of novae**.

Light curve modelling of the *Swift* light curve of RS Oph was performed by Hachisu et al. (2007), who assume that the optically thick wind has stopped with the start of the SSS phase. The high-amplitude variations are neglected in the light curve model.

During the SSS phase of RS Oph, periodic variations of ∼ 35 seconds were present in the *Swift* and *XMM-Newton* X-ray light curves (Osborne et al. 2006c,b; Ness et al. 2007b). The same 35-s period was also found in *Swift* observations of KT Eri, leading Beardmore et al. (2010) to
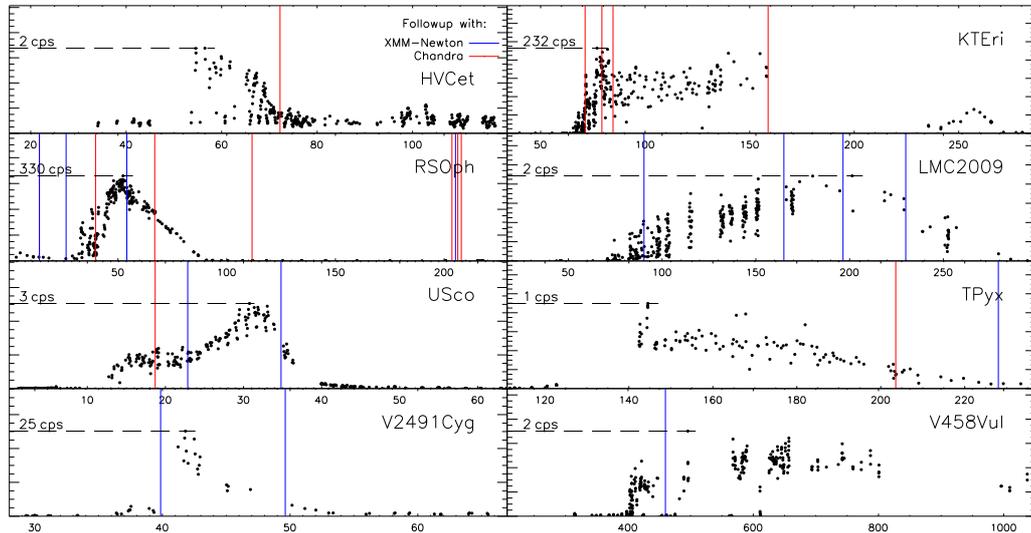
Figure 2. *Swift* X-ray monitoring observations of novae result in unprecedented long-term light curves. The best 8 examples are shown with the name of each nova given in the top right of each panel and the maximum observed count rate (cps=counts per second) marked in the left above a horizontal dashed line. The horizontal time axes are different for each novae. A large range of time scales and brightness levels have been encountered. The coloured vertical lines indicate the times of *XMM-Newton* (blue) and *Chandra* (red) observations. Optimal times and exposure time for deeper followup observations can be determined from the *Swift* monitoring, making *XMM-Newton* and *Chandra* observations a lot more valueable.

conclude that it is not related to rotation but rather intrinsic, e.g., nuclear burning instabilities. The complete set of *Swift* X-ray spectra taken during the SSS phase of RS Oph were studied in detail by Osborne et al. (2011). The low-resolution *Swift* spectra were modelled with the same atmosphere code, in which a set of fixed parameters was chosen in addition to which the evolution of effective temperature, line-of-sight absorption (N_H), radius, and luminosity was studied. As in the case of the hydro model used by Vaytet et al. (2011), a highly complex model fitted to low-resolution spectra needs to be constrained by high-quality grating spectra, if available. However, currently, no atmosphere model has so far been found that reproduces the grating spectra in all details. For example, Nelson et al. (2008) present a preliminary model using the same code used by Osborne et al. (2011), and it does not reproduce the grating data. The assumed fundamental physics may thus be wrong, but the approach is to consider only relative changes, and Osborne et al. (2011) found that the early variability phase was not only variable in brightness but also in temperature and absorption.

A similar approach to find the underlying physical changes that lead to spectral changes during the SSS phase were presented by Page et al. (2010) using the monitoring data of the fast nova V2491 Cyg (see bottom left panel of Fig. 2). Instead of an atmosphere model, a simple
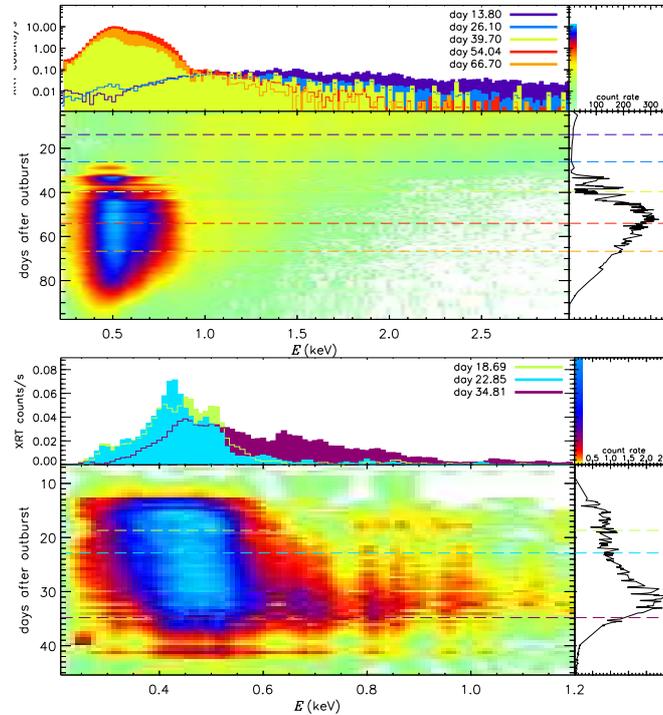
Figure 3. Spectral evolution maps of the *Swift* monitoring campaign of RS Oph (top) and U Sco (bottom). In each plot, the top panel displays spectra extracted from time intervals corresponding to the horizontal dashed lines of the same colours in the time map below and in the light curve to the right (rotated by 90°). The times when grating observations were taken have been chosen. The central panel illustrates the spectral time evolution with elapsed observing time along the vertical axis and wavelength across, on the same scales as the light curve in the right and the spectra on top, respectively. The brightness is colour coded, and for each colour, the corresponding count rate can be derived from the colour bar in the top right. *The data of RS Oph are the same as used by Osborne et al. (2011) and have kindly been provided by Drs. Kim Page and Andrew Beardmore of the University of Leicester.*

blackbody fit was used, yielding the same parameters, effective temperature, N_H, radius, and luminosity, again only inspecting the relative changes, even though the underlying physics of the model are not fully correct.

The recurrent nova U Sco had been overdue to explode again in 2009 (Schaefer 2005) and was monitored in the optical very closely until the outburst was finally discovered in January 2010 (Schaefer et al. 2010). Its particular importance arises from the fact that the binary system is seen edge on, yielding total eclipses (Schaefer 1990). *Swift* monitoring started immediately after outburst, with the first observation only 1.2 days after outburst. No detection in X-rays was found until the onset of the SSS phase (Schlegel et al. 2010). Consecutive *Swift* observations were centred around predicted eclipse times, but with a series of short snapshots, eclipses in X-rays

were at most suggestive from phase-folded count rates (Osborne et al. 2010) from several cycles. A continuous *XMM-Newton* observation indicated X-ray dips rather than an eclipse (see Fig. 9 in Section 4.3). After ~day 30, the *Swift* count rates showed much clearer eclipses, and a second *XMM-Newton* observation was scheduled which then also contained a clear X-ray eclipse. The entire *Swift* light curve is shown in the third panel of the left column in Fig. 2 and the spectral evolution in the bottom panel of Fig. 3. Clearly recognized can be a continuous increase in temperature with time.

4.2 Pre-*Swift*, *XMM-Newton/Chandra* observations

The very first X-ray grating spectrum of a nova, taken on 2000 February 14 was of V382 Vel, which was found in the SSS state in a *Chandra* ACIS observation of 1999, December 30 (Burwitz et al. 2002). The resulting spectrum was much fainter than expected, indicating that the nova had turned off within only 2.5 months. The grating spectrum was still useful as it displayed post-outburst nebular emission lines that had never been seen before. Ness et al. (2005) inspected and analysed the data using an emission measure distribution model. The line profiles revealed double peaks indicative of different kinematic components of the nebular plasma. Weak continuum was seen that could arise from a 3×10^5-K WD, indicating that it had not yet cooled down after the outburst. Under the assumption of collisional equilibrium in a low-density plasma as in stellar coronae, the distribution of kinetic (electron) temperature could be reconstructed from line ratios. From the inferred temperature distribution and systematic deviations of predicted and measured lines fluxes, the elemental abundances could be derived. Although the nova had gone through an earlier so-called Fe-curtain phase in the UV (Shore et al. 2003), the X-ray spectrum contains no Fe lines. The abundance diagnostics confirmed that Fe was at least 4% underabundant with respect to oxygen. Ness et al. (2005) argue that instead of underabundant Fe, the elements that produce the observed emission lines are overabundant. Two more *Chandra* observations of V382 Vel were taken with the ACIS, without a grating, and with the low CCD resolution. Fading emission lines were visible (Burwitz et al. 2002).

A few months later, the nova V1494 Aql offered another opportunity to study a nova evolution with *Chandra*. Without any knowledge about how bright the nova may be in X-rays, a blind shot was taken with the ACIS on day 134 after outburst, and the 5-ks observation yielded a hard spectrum with two resolved emission lines, but no signs of SSS emission (see Fig. 4). Fortunately, significant X-ray emission was present already before the SSS phase started, so more observations in ~ 3 months intervals yielded secure results with good perspectives for eventually finding SSS emission. On day 248, clear indications for SSS emission arose, albeit still not quite as bright as in other novae. On day 300, the grating was then employed, yielding the first SSS spectrum of a nova in high resolution. This spectrum is different than expected, showing continuum plus emission lines. Four days later, a deeper exposure was taken, yielding a similar spectrum, thus the SSS spectrum is not an atmospheric spectrum as expected. It may be related to the high system inclination angle (Barsukova & Goranskii 2003; Ness et al. in preparation, and Fig. 11). To this date, no satisfactory spectral model could be found. For discussion also on timing analysis, I refer to Rohrbach, Ness & Starrfield (2009). Without any information how long the SSS phase may
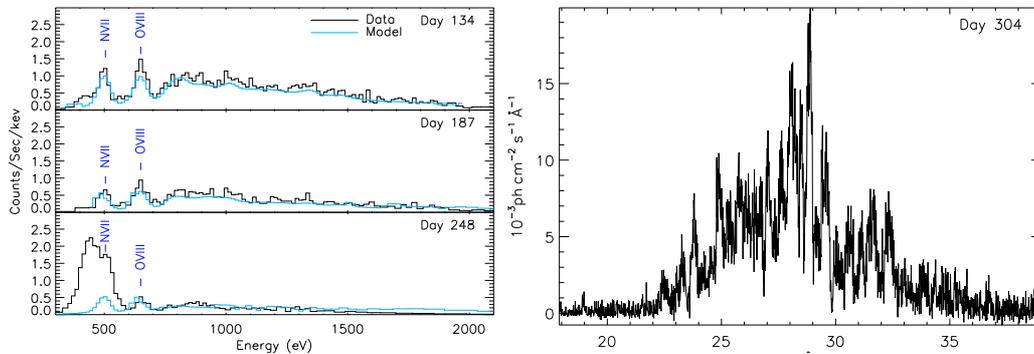
Figure 4. Illustration of an observing strategy without *Swift*. During the early evolution of V1494 Aql, while it was not clear what would be seen, short (5-6 ks observations) with the ACIS-I were taken (left panel; figure taken from Rohrbach et al. 2009; for more details see there). The nova was still too faint for the gratings but the faint pre-SSS ACIS spectrum originated from optically thin thermal plasma that can be parameterised by the electron temperature; see model plotted in light blue. On day 248 after outburst, a clear SSS component was detected, justifying longer grating observations that were taken 2 months later (right panel).

last, the next observation was taken one year later, but the nova had already turned off, yielding a weak detection only in the zero-th order of the grating observation. Five years later, *Swift* observed again with no further detections (Section 4.1).

Nova V4743 Sgr (2002) was also studied without additional information from other X-ray observatories. Again, in order to avoid non-detections in a long grating observation, a first, short, 5-ks, snapshot was taken in November 2002, two months after the outburst. Again, a clear detection was found, but no SSS spectrum. The nova was then not visible for 4 months, but as soon as it came back from behind the sun, a grating spectrum was taken (180.4 days after outburst), yielding the first really bright SSS spectrum with continuum and deep absorption lines from highly ionised species (Ness et al. 2003). A graphical illustration of the spectral evolution during this observation is shown in Fig. 5.

The observation starts with high-amplitude periodic variations, and eight clean cycles are marked with different colours in the light curve, turned around by 90°, in the right panel of Fig. 5. These eight cycles have been used to create a phase-folded light curve and corresponding spectral map, shown in the middle plot. The two spectra in the top are integrated over all phase minima and phase maxima, respectively, showing that the minima spectra are systematically softer. These periodic X-ray variations have been seen in all X-ray observations, including those taken during post outburst. Detailed timing analyses have been carried out by Leibowitz et al. (2006); Dobrotka & Ness (2010), discovering the double nature of the frequency during the SSS phase, which later merges into a single frequency (Dobrotka & Ness 2010).

About 2 hours before the end of the observation, the count rate suddenly dropped from 40-60
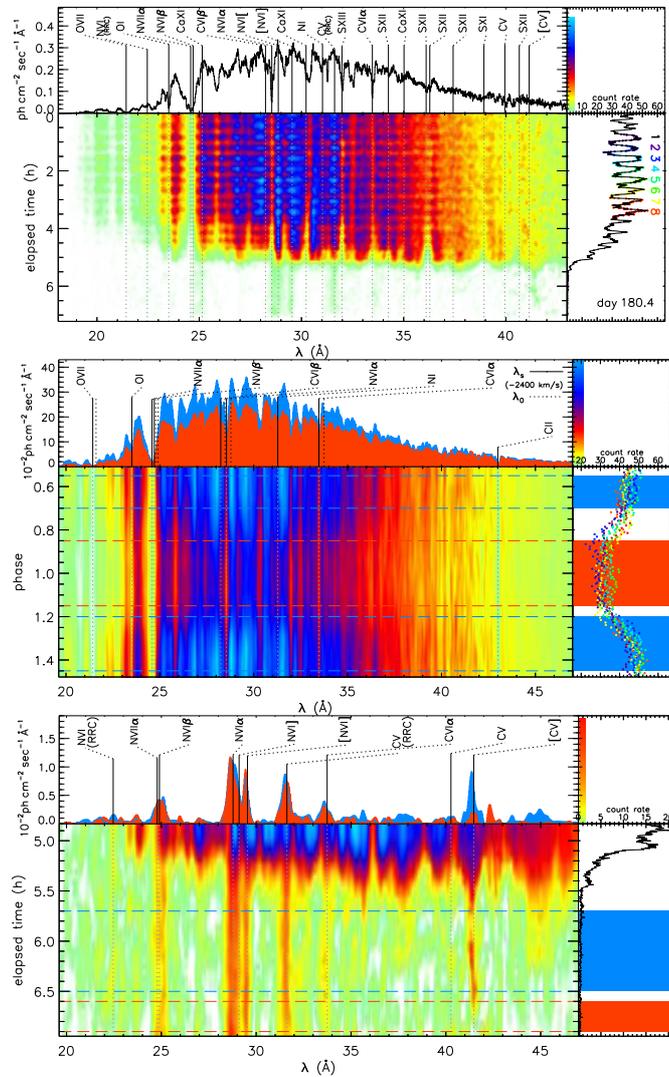
Figure 5. Spectral evolution maps of a *Chandra* observation of V4743 Sgr on day 180.4 after outburst, each plot illuminating a different aspect using the same illustration concept as explained in Fig. 3. In the top, the evolution over the entire observation is shown. After a phase of periodic variations (period 1313.6 seconds, eight clean cycles are marked), a steep decline sets in, leaving behind weak emission lines. The spectrum can be seen to first fade at shorter wavelengths. Spectral changes along the periodic variations are illustrated by the phase-folded plot in the middle, folding the eight cycles marked in the top. The colours of the plot symbols in the right indicate from which cycle the corresponding data points originate. In the bottom, the transition from bright to faint is illustrated. The forbidden line of C v at ∼ 41.5 Å and some broader features around 37 Å and 45 Å seem to fade with time.

counts per second to nearly zero within a very short time. No technical fault was identified, but a physical cause for such a steep decline was not easily found. At that time, the high-amplitude variations during the early SSS phase described above had not yet been discovered, and it appears plausible that this decline was in fact the first time this phenomenon was seen.

In the top plot, one can see that the harder part of the spectrum, shortward of ∼ 28 Å, started earlier with the decline than the softer part, and that emission lines were left behind, both reported by Ness et al. (2003). The evolution of the faint emission lines after the decline is illustrated in the bottom, and one can see that some emission lines are variable. The forbidden line of C v ($1s^2\,{}^1S_0$–$1s2p\,{}^3S_1$) at 41.47 Å is much stronger than the $1s^2\,{}^1S_0$–$1s2p\,{}^1P_1$ resonance line at 40.27 Å. While at about 5.7 hours after the start of the observation, the [C v] line disappears, it reappears between 6.0 and 6.6 hours, at first red shifted and then gradually changing to being blue shifted. If the [C v] emitting material originated from plasma that co-rotates with the WD at 2400 sec spin period, red/blue shifts of ±0.15 Å implied an orbital radius of 3 R$_\odot$. It bears closer investigation, however, why a plasma so far away would not produce any resonance line emission.

The sudden decline triggered an *XMM-Newton* observation only two weeks later (day 196.1 after outburst), in which the source was as bright as before the decline started (Orio et al. 2003), indicating that it was a transient phenomenon, strengthening the link to the early high-amplitude variability phase. Denser monitoring than for V1494 Aql was chosen with three more observations on days 301.9, 371, and 526.1 after outburst, and all yield the same general spectrum with some changes in temperature and in several details, but no further decline as on day 180.6 was seen.

All five SSS spectra of V4743 Sgr were modelled by Rauch et al. (2010) using the Tübingen Model Atmosphere Package (TMAP), a non-LTE atmosphere model that is optimised for hot WDs. The evolution of the effective temperature was described to have been reached on day 196.1, after which it remained stable at least until day 371. A massive WD of 1.1-1.2 M$_\odot$ was deduced, and the photosphere was found to be nitrogen-rich and carbon-deficient, indicative of CNO cycle processed material. Under the assumption that the observed photospheric emission arises from the surface of the WD, it was concluded that some of the accreted material was not ejected and remained instead on the WD. Towards later observations, a reduced nitrogen abundance was derived, implying that new, N-poorer, material was present that may come from the companion via renewed accretion.

These conclusions may depend to some degree on the assumptions that, in spite of the complexity of the TMAP code, must still be considered somewhat simplified. Ness et al. (2011) argued that assumptions such as hydrostatic equilibrium and a plane parallel geometry are only valid in isolated hot WDs, for which the TMAP code is designed, but not in expanding nova ejecta. The blue shifts of the atmospheric absorption lines in the X-ray grating spectra give direct witness of the continued expansion and thus a non-static environment. In the TMAP model, Rauch et al. (2010) introduced an artificial blue shift to better reproduce the data, but the entire atmosphere structure may be fundamentally different in an expanding environment. Attempts

to model also the expansion in non-LTE radiative transport calculations have been made in the PHOENIX code (see, e.g., Hauschildt et al. 1992; Hauschildt & Baron 1999). Clearly, the complexity increases even further, but the X-ray grating spectra are of sufficient quality to use such approaches. The PHOENIX code was originally designed to model UV spectra, but has later been expanded to the X-ray regime (Petz et al. 2005) and improved by van Rossum (2009) with first results shown by van Rossum & Ness (2010), who found that atmosphere models that account for the expansion yield vastly different results from static models. Most recently, van Rossum (2012) presented a full description of a new model, based on PHOENIX, called "Wind-Type" (WT) SSS Nova Model, that will be made publicly available. The same five grating spectra of V4743 Sgr have been modelled, yielding different principal parameters than those found by Rauch et al. (2010). The effective temperatures are generally lower while N_H is higher. The values found by van Rossum (2012) are in better agreement with Galactic neutral hydrogen maps of Kalberla et al. (2005) and Dickey & Lockman (1990) as implemented in the HEASARC Galactic N_H tool[1] yielding 1.1×10^{21} and 1.4×10^{21} cm^{-2}, respectively. The differences between van Rossum (2012) and Rauch et al. (2010) can partly be explained by a different approach in determining N_H, but the main difference is caused by two additional parameters, v_∞ and $\dot{M}$ in van Rossum (2012), parameterising the expansion. More work will be needed to investigate the effects of non-solar abundances. Well constrained model parameters will guide theoretical nova evolution models. The low-resolution spectra taken during *Swift* monitoring can be used to interpolate the models that have been constrained in detail by 2-3 grating spectra.

4.3 *Swift*-assisted *XMM-Newton/Chandra* observations

The greatest difficulty in getting grating spectra during the SSS phase is finding the right moment. This has been overcome with the use of *Swift* to get short snapshots over much shorter time intervals (see Section 4.1). The *Swift* count rates were used to calculate the required grating exposure times.

The first time that the potential of *Swift* for nova studies were systematically explored was during the 2006 outburst of the recurrent, symbiotic, nova RS Oph. Initial *Swift* observations established an extremely high X-ray brightness level, with severe pile up in the photon counting mode. There was no doubt that short grating observations would be highly informative, and simultaneous *XMM-Newton* and *Chandra* observations were organised to take place only two weeks after outburst. While *Swift* monitoring continued, grating observations were taken whenever significant changes in brightness and spectral shape were seen with *Swift*, yielding a total of three *XMM-Newton* and three *Chandra* observations before the end of the SSS phase (see 2nd panel in left row of Fig. 2). The nova remained interesting even after it turned off, and more grating observations were taken. An overview of the grating observations, given by Ness et al. (2009b), is reproduced in Fig. 8. The first two spectra were extracted from the two grating arms of

---

[1] http://heasarc.nasa.gov/cgi-bin/Tools/w3nh/w3nh.pl

the *Chandra*/HETGS, the Medium Energy Grating (MEG) and the High Energy Grating (HEG). These observations were taken simultaneously with the *XMM/RGS* (third spectrum in Fig. 8).

The top four spectra in Fig. 8 were taken during the shock phase, before the SSS phase started, when the nova ejecta ran through the dense stellar wind of the giant companion star, dissipating significant amounts of kinetic energy during shocks, that was partially converted to X-ray emission. The X-ray spectrum is that of a plasma in collisional equilibrium, evidenced by line ratios of He-like emission lines of Mg (Nelson et al. 2008). Two different groups have analysed the same spectra in different ways: Nelson et al. (2008) applied an `xspec` (Arnaud 1996) multi-temperature model with solar abundances, needing 4 temperature components. Ness et al. (2009b) used two approaches, first the same as Nelson et al. (2008) but with variable abundances, needing then only three temperature components. High overabundance of Mg and Si and underabundance of Fe, relative to oxygen, were found. Since a plasma of three distinct temperature components is not necessarily physically realistic, Ness et al. (2009b) also applied the same method already used for V382 Vel assuming a continuous temperature distribution (see above and Ness et al. 2005) and found the same general abundance trends, but with better constraints of N and S. Comparison of the abundances with those in single giants revealed considerable anomalies suggesting that the companion in RS Oph has changed substantially by the continued mass loss via accretion. Alternatively, these abundances would reflect the composition of the WD which would question the system to be a SN Ia progenitor which requires a carbon-oxygen rich (CO) WD while the observed abundances in the X-ray plasma would indicate more an oxygen-neon (ONe) white dwarf. The difference in nuclear binding energy between α elements (such as neon, magnesium, silicon) and iron is not sufficient to disrupt the WD while nuclear fusion chain reactions starting from carbon, as found in a CO WD, produce more energy.

The SSS phase of RS Oph may have started during the *XMM-Newton* observation taken on day 26.1 in which Nelson et al. (2008) observed the appearance of a new soft component. While the high-energy part of the spectrum (fourth panel in Fig. 8) could be modelled with the same approaches of collisional plasma as for day 13.8 (Ness et al. 2009b), the new soft component between $\sim 24 - 31$ Å coincides in wavelength with the soft tail of the later SSS phase (see fourth and fifth panels in Fig. 8). In a low-resolution spectrum, the new component would have been interpreted as first signs of atmospheric emission, and a blackbody fit to the simultaneous *XMM-Newton/MOS* spectrum indeed yields a good fit. However, in the high-resolution RGS spectrum, several unknown overlapping emission lines can be seen, quite atypical of SSS emission. An illustration of the time evolution of the appearance of the new soft component during the observation is given with Fig. 6. Only two lines of N vi (1s-2p triplet) at 28.8-29.5 Å and N vii (1s-2p doublet) plus N vi (1s-3p) at ~ 25 Å can be identified while all other features are of unknown origin. Nelson et al. (2008) speculate these may be highly blue-shifted 1s-3p and 1s-4p lines of C vi, but the principle C vi 1s-2p line at 33.8 Å is not present (see Fig. 6), and also the C abundance was argued in other context of the same article to be extremely low. From Fig. 6 it can be seen that the unknown emission features were present for only 40-50 minutes (between the two horizontal dashed red lines), suggesting these may be instable transitions, e.g., between excited states. A conclusive interpretation of the day-26.1 spectrum of RS Oph is still outstanding but important as it may hold clues of the transition into the SSS phase.
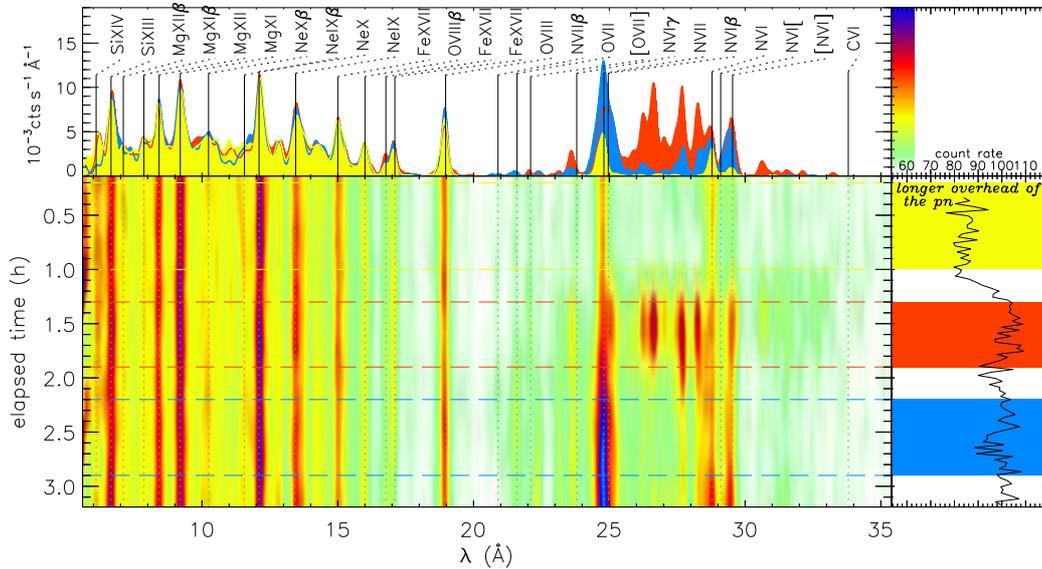
Figure 6. Spectral evolution map of *XMM-Newton* observations of RS Oph on day 26.1 (see Fig. 3 for description of the illustration concept). While the spectrum shortward of 20 Å remains constant, the rise in total flux about one hour after the start of the observation is owed to a new soft component between 24-31 Å, first described by Nelson et al. (2008). The spectrum of the new soft component is not typical SSS emission but consists of unknown emission lines.

A few days later, *Swift* observed a steep rise into the SSS phase, and a *Chandra* LETG observation was scheduled which fell, however, into an unanticipated low state that occurred soon after. Nevertheless, an extremely well exposed spectrum was obtained. Continued *Swift* monitoring allowed scheduling of two more grating observations during the peak and decline of the SSS phase (see Fig. 2). The time evolution of this observation is illustrated in Fig. 7. On shorter time scales also, the nova was found highly variable. A 1000-s delay between brightness and hardness light curves in the day 39.7 (see right panel of Fig. 7) observation led Ness et al. (2007b) to conclude that photoionisation of neutral oxygen led to variations in transparency, allowing more (harder) X-ray light to escape when oxygen is ionised. Considerable reductions in the depth of the neutral oxygen edge towards the later observations support this conclusion.

Based on the *Swift* light curve of the famous recurrent nova U Sco, shown in the third panel of the left column in Fig. 2 and the bottom plot in Fig. 3, an initial *Chandra* observation was scheduled on day 18.7 after outburst but was not centred around eclipse. Later, on day 22.9, a longer continuous *XMM-Newton* observation was scheduled that resolved the details of the X-ray brightness during optical eclipses. Guided by the contemporaneous OM light curve that clearly showed an eclipse, Ness et al. (2012) showed that dips occurred between quadratures (phases -0.75 to 0.25; see left panel in Fig. 9). A few days later, the *Swift* count rates showed clear eclipses, and a second *XMM-Newton* observation was scheduled to resolve the details (see right panel in Fig. 9). The X-ray spectrum during the SSS phase was atypical again, with strong emission lines
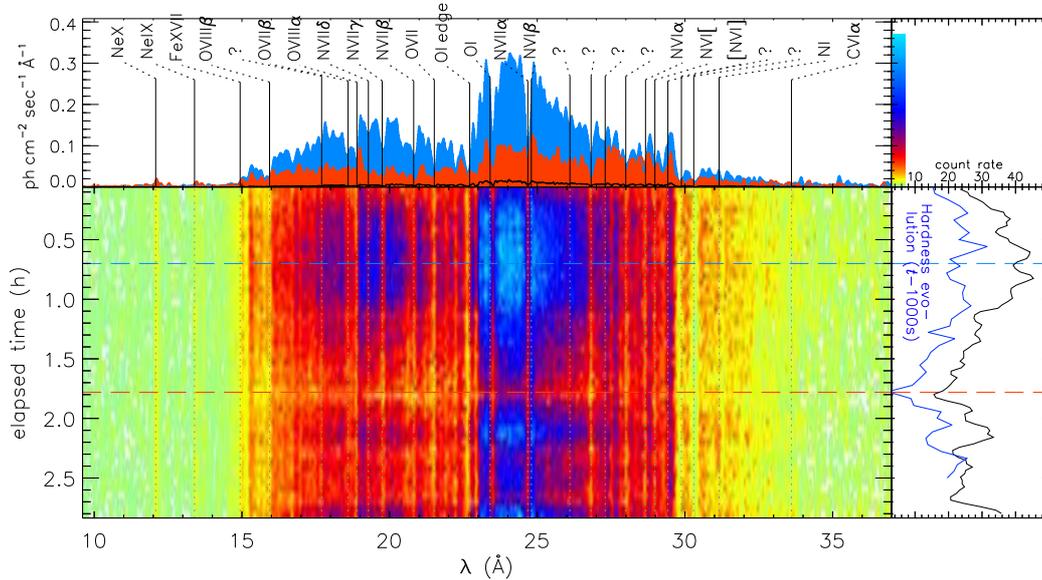
Figure 7. Spectral evolution map, as explained in Fig. 3, for the *Chandra* observation taken during the high-amplitude variability phase of RS Oph, on day 39.7. A 1000-second shift of the hardness light curve versus brightness discovered by Ness et al. (2007b) is illustrated in the right by the shifted hardness light curve in blue.

on top of blackbody-like continuum, resembling the proto typical SSS Cal 87 in the LMC, which is also an eclipsing system. Ebisawa et al. (2010) discussed the possibility that the accretion disk in Cal 87 blocks the central emission from the WD, and all observable X-ray emission originates from Thomson scattering within the Accretion Disk Corona (ADC). Additional resonance line scattering can produce the observed emission lines. To transfer these conclusions to U Sco, an accretion disk must already have been present or in the process of re-establishment. The dips in X-rays can be explained by neutral clumpy material within an accretion stream from the companion star. Neutral gas is transparent to UV/optical light but opaque to X-rays. Once the accretion disk has flattened, no more dips are seen in X-rays.

The very fast nova V2491 Cyg entered the SSS phase just a bit more than a month after outburst. Guided by the *Swift* snapshots (see bottom left panel in Fig. 2), two *XMM-Newton* observations were triggered in short succession, on days 39.9 and 49.6, both extremely well exposed. Without *Swift*, this quick evolution could not have been followed. Significant X-ray variability was found on day 39.9 (Ness et al. 2011, see Fig. 10). The absorption lines were highly blue shifted indicating high expansion velocities. Ness et al. (2011) also showed that currently publicly available atmosphere models are not sufficient to reproduce these high-quality spectra. Preliminary PHOENIX atmosphere models to the V2491 Cyg spectra were presented by van Rossum & Ness (2010), using a combination of a hydrostatic core and a hydrodynamic expanding envelope. The additional expanding envelope yields a clearly better fit to the data, but the large majority of absorption lines are not reproduced. Pinto et al. (2012) developed a
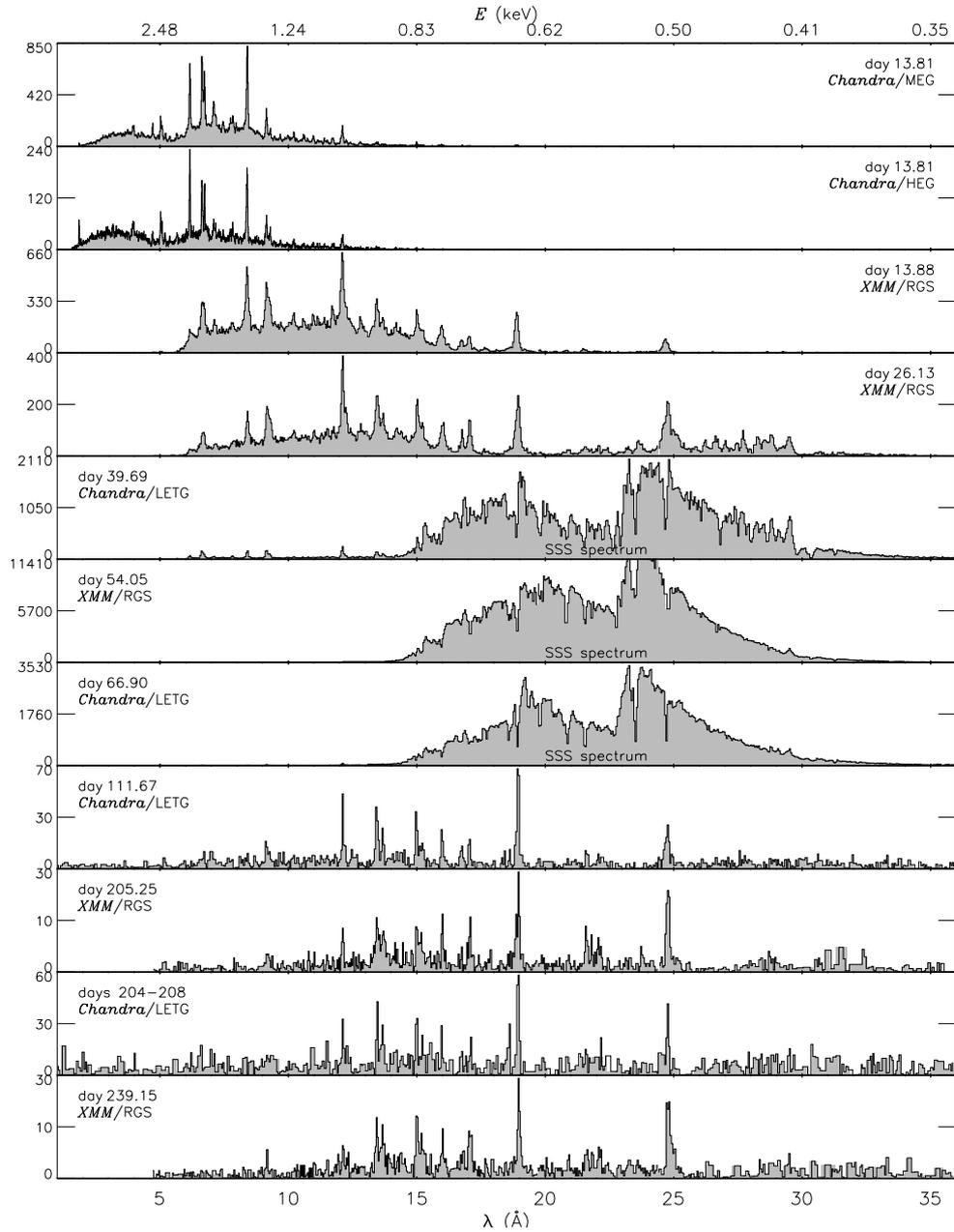
Figure 8. All grating observations taken during the 2006 outburst of RS Oph (figure taken from Ness et al. 2009b).
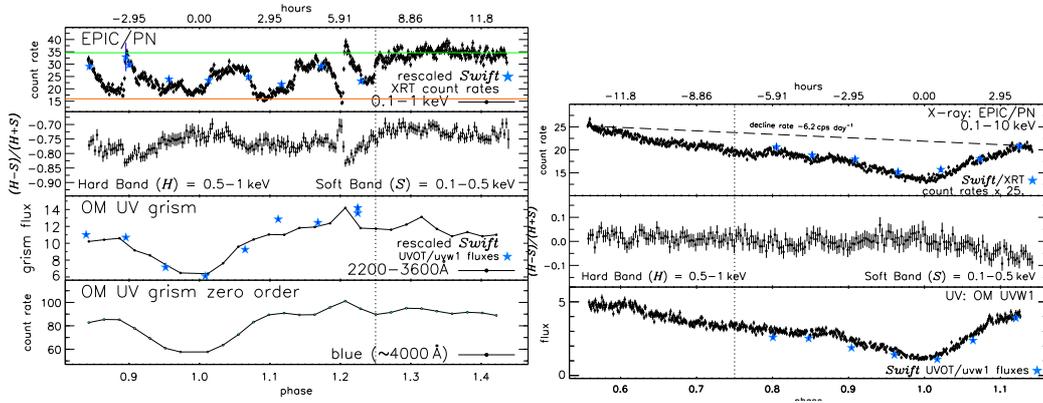
Figure 9. XMM-Newton X-ray and UV light curves of U Sco, centred on eclipses (taken from Ness et al. 2012). In the earlier observation (left), X-ray dips and a clean eclipse in UV and optical are seen, while in the later observation (right), also the X-ray light contains a clean eclipse. Ness et al. (2012) interpret these changes as signature of the re-establishment of accretion during the SSS phase.
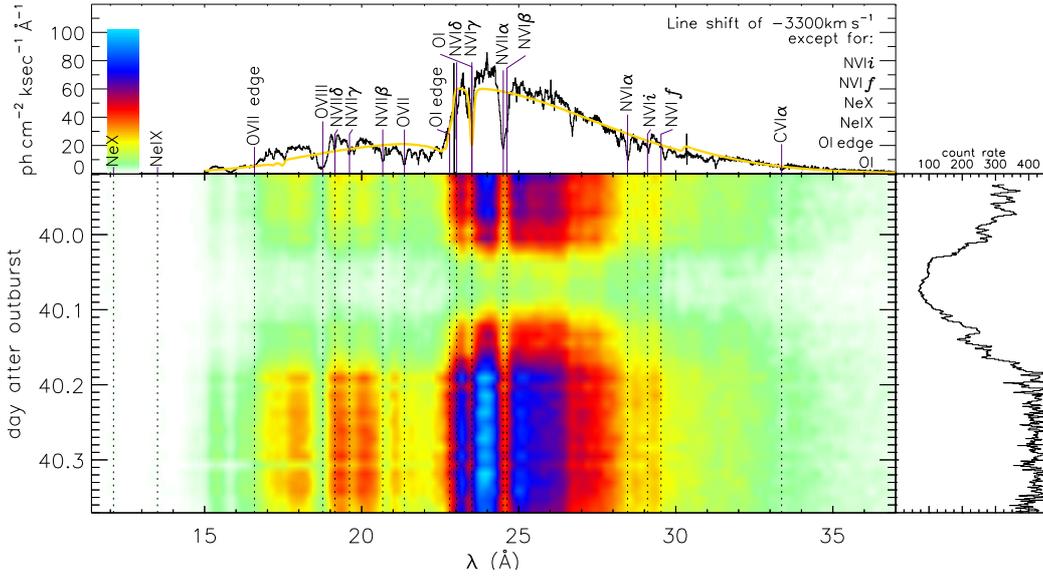
Figure 10. Spectral evolution map following the same concept as Fig. 3, illustrating spectral changes along the variability in the *XMM-Newton* observation of V2491 Cyg on day 39.9. In the top panel, the total RGS spectrum is shown with a blackbody fit to the continuum component.

new approach using a multicomponent SPEX (Kaastra et al. 1996) model, consisting of emission and absorption components, but this approach also did not reproduce the spectra in a formally satisfactory way.

The classical nova KT Eri was followed with four *Chandra* observations. The nova was extremely bright (Bode et al. 2010) enabling short exposures of only a few 10^3 seconds to obtain extremely well exposed spectra (Ness et al. 2010). Again, these grating spectra are extremely complex.

5. Conclusions

While results from individual observations have already been discussed in the previous sections, I focus here on more general conclusions that can be drawn from the entirety of all observations.

5.1 Pre- and Post-SSS phase

Originally, novae were only expected to be X-ray sources during their SSS phase, when the photospheric radius had receded into the nuclear burning regions near the surface of the WD. However, already the earliest X-ray observations of novae have revealed pre-SSS X-ray emission, e.g., in V838 Her (O'Brien et al. 1994) or V1974 Cyg (Krautter et al. 1996). Plasma models to the low-resolution data indicate that the emission arises from a collisional plasma and is suspected to originate in shock fronts within the ejecta (e.g., Brecher et al. 1977). An "interacting winds" model has been developed by O'Brien et al. (1994) and was refined by Lloyd et al. (1995) for the specific case of V838 Her. They argued that the shock-heating must take place as a result of the interaction of different components *within* the ejecta.

The much increased sample of X-ray observed novae with the new-generation X-ray observatories gives an idea of the frequency of early hard emissions. Out of 27 novae that have been observed with *Swift* within the first 100 days after outburst with at least two observations, 11 were detected but without an SSS component in the first observation and 17 in the second observation. Thus about half of all novae display pre-SSS X-ray emission.

The interacting winds model predicts inhomogeneities within the ejecta, and these may have left their footprints also in the later SSS grating spectra that contain complex absorption line profiles indicating different velocity components (see, e.g., Ness et al. 2011). It needs to be kept in mind that the early spectra of RS Oph have a different origin with shocks between the ejecta and the stellar wind of the companion, that is less dense in main sequence companions. This produces much more X-ray emission than intra-ejecta shocks. Owing to their intrinsic faintness, intra-ejecta shock spectra have never been observed with an X-ray grating.

Post-SSS grating spectra were taken of V382 Vel and of RS Oph, both yielding faint emission line spectra. While V382 Vel contains multiple velocity components, the spectral lines in RS Oph are single. Both spectra can be modelled by collisional plasma models, which is not necessarily trivial with grating spectra. The post-SSS emission phase likely originates in radiatively cooling nebular ejecta (e.g., Ness et al. 2005) which can be highly non-solar in composition.

5.2 SSS phase

The new observations during the SSS phase have revealed a number of unexpected complications such as high-amplitude variations during the early SSS phase (see Section 4.1), extremely complex high-resolution spectra, and a high degree of diversity.

The expected form of an SSS spectrum was an atmospheric absorption line spectrum. However, the first ever nova that was observed during the SSS phase with a grating, V1494 Aql, displayed a completely different spectrum (see right panel of Fig. 4), and spectral modelling was so far unsuccessful (Rohrbach et al. 2009). The second observed nova SSS spectrum, of V4743 Sgr, complied better with expectations (see Fig. 5), but the light curve was violently variable with the mysterious decline that only years later can be seen in the context of the early variability phase. The high degree of diversity was unexpected, and only with more observations, some similarities were found, for example a remarkable similarity between the SSS spectra of RS Oph and V2491 Cyg (Ness et al. 2011). Spectral modelling of SSS spectra still leaves too many doubts to lead to conclusive results. Not a single approach has so far led to satisfactory reproduction of the observed spectra in a statistical sense. Attempts were made with:

1. The non-LTE WD atmosphere model TMAP (Rauch et al. 2010)
2. The expanding radiative transfer model based on PHOENIX (van Rossum 2012)
3. A multicomponent SPEX model (Pinto et al. 2012).

TMAP is currently the best tested approach and is available to the scientific community, however, the expansion of the absorbing plasma, proven by the observed line blue shifts, invalidates the assumptions of hydrostatic equilibrium and plane parallel geometry. An approach to compute radiative transport in a co-moving frame has been implemented in the PHOENIX code, and van Rossum & Ness (2010) have shown that hydrostatic and hydrodynamic models lead to different spectra, and adjustments to observed spectra lead to different key parameters. The conclusions drawn from TMAP modelling are therefore to be treated with care. The PHOENIX code may be more promising as demonstrated by van Rossum (2012). Although currently only models with solar abundances are available, already good agreement between models and data has been found. These models will be publicly available and could be used to parameterise individual grating spectra and then using these models to interpolate along the low-resolution *Swift* spectra to get the full evolution of the atmosphere parameters at the time density of the *Swift* monitoring. The approach by Pinto et al. (2012) of combining emission- and absorption components in a self-consistent way may be a promising alternative, but one has to be careful to use the large number of degrees of freedom wisely.

The studies of U Sco have given more clues, as the eclipsing system displayed an SSS spectrum that resembles the also eclipsing proto-typical SSS Cal 87 (Ebisawa et al. 2010). There is reason to believe that high-inclination systems contain stronger emission line components with less-pronounced absorption lines than low-inclination systems. In Fig. 11, 14 grating SSS spectra are shown in comparison. The light blue lines guide the eye that all sources contain photospheric
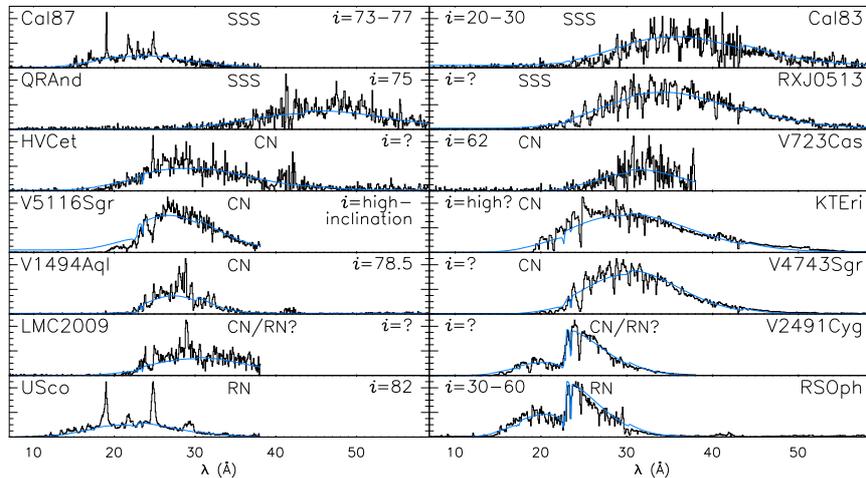
Figure 11. High-resolution X-ray spectra in arbitrary flux units of supersoft sources that contain emission lines without absorption features (left column) and those that consist of continuum and absorption lines (right column). Inclination angles i from the literature are given if known. The blue thin lines are black-body curves, indicating the presence of photospheric emission in all cases. The labels SSS, CN, and RN denote persistent supersoft sources, classical novae, and recurrent novae, respectively. More details will be presented in an upcoming paper by Ness et al.

continuum emission that has the shape of a blackbody. More detailed discussion will be presented in an upcoming paper (Ness et al., in preparation). An inclination-angle dependence indicates asymmetric ejecta and possibly the presence of renewed accretion. If we are dealing with clumpy accretion, the early variability phase could be explained as temporary ocultations of the central source that cease when a flatter accretion disk has formed.

References

Arnaud K. A., 1996, in Jacoby G. H., Barnes J., eds, ASP Conf. Series, Astronomical Data Analysis Software and Systems V, Vol. 101, p. 17

Balman S., Krautter J., Ögelman H., 1998, ApJ, 499, 395

Barsukova E. A., Goranskii V. P., 2003, Astr. Lett., 29, 195

Beardmore A. P. et al., 2010, The Astronomer's Telegram, 2423, 1

Bode M. F., Evans A., 2008, in Bode, M. F., Evans, A., eds, Classical Novae, Cambridge University Press

Bode M. F. et al., 2006, ApJ, 652, 629

Bode M. F. et al., 2010, The Astronomer's Telegram, 2392, 1

Brecher K., Ingham W. H., Morrison P., 1977, ApJ, 213, 492

Burrows D. N. et al., 2005, Space Sci. Rev., 120, 165

Burwitz V., Starrfield S., Krautter J., Ness J.-U., 2002, in Hernanz M., José J., eds, AIP Conf. Proc.: Classical Nova Explosions, Vol. 637, American Institute of Physics, p. 377

den Herder J. W. et al., 2001, A&A, 365, L7

Dickey J. M., Lockman F. J., 1990, ARAA, 28, 215

Dobrotka A., Ness J., 2010, MNRAS, 405, 2668

Ebisawa K., Rauch T., Takei D., 2010, AN, 331, 152

Gallagher J. S., Starrfield S., 1976, MNRAS, 176, 53

Greiner J., Hasinger G., Kahabka P., 1991, A&A, 246, L17

Hachisu I., Kato M., Luna G. J. M., 2007, ApJ, 659, L153

Hartmann H. W., Heise J., 1997, A&A, 322, 591

Hauschildt P. H., Baron E., 1999, J. Computational and Applied Mathematics, 109, 41

Hauschildt P. H., Wehrse R., Starrfield S., Shaviv G., 1992, ApJ, 393, 307

Kaastra J. S., Mewe R., Nieuwenhuijzen H., 1996, in Yamashita K., Watanabe T., eds, UV and X-ray Spectroscopy of Astrophysical and Laboratory Plasmas, p. 411

Kahabka P., Pietsch W., Hasinger G., 1994, A&A, 288, 538

Kahabka P., van den Heuvel E. P. J., 1997, ARA&A, 35, 69

Kalberla P. M. W., Burton W. B., Hartmann D., Arnal E. M., Bajaja E., Morras R., Pöppel W. G. L., 2005, A&A, 440, 775

Krautter J., 2002, in Hernanz M., José J., eds, AIP Conf. Series, Vol. 637, Classical Nova Explosions, p. 345

Krautter J., 2008, in Evans A., et al., eds, ASP Conf. Series, Vol. 401, RS Ophiuchi (2006) and the Recurrent Nova Phenomenon, p. 139

Krautter J., Ögelman H., Starrfield S., Wichmann R., Pfeffermann E., 1996, ApJ, 456, 788

Leibowitz E., Orio M., Gonzalez-Riestra R., Lipkin Y., Ness J., Starrfield S., Still M., Tepedelenlioglu E., 2006, MNRAS, 371, 424

Lloyd H. M., O'Brien T. J., Bode M. F., 1995, Ap&SS, 233, 317

Long K. S., Helfand D. J., Grabelsky D. A., 1981, ApJ, 248, 925

Nelson T., Orio M., Cassinelli J. P., Still M., Leibowitz E., Mucciarelli P., 2008, ApJ, 673, 1067

Ness J. et al., 2009a, AJ, 137, 4160

Ness J., Drake J. J., Starrfield S., Bode M., Page K., Beardmore A., Osborne J. P., Schwarz G., 2010, The Astronomer's Telegram, 2418, 1

Ness J. et al., 2009b, AJ, 137, 3414

Ness J. et al., 2011, ApJ, 733, 70

Ness J. et al., 2012, ApJ, 745, 43

Ness J., Schwarz G., Starrfield S., Osborne J. P., Page K. L., Beardmore A. P., Wagner R. M., Woodward C. E., 2008, AJ, 135, 1328

Ness J., Schwarz G. J., Retter A., Starrfield S., Schmitt J. H. M. M., Gehrels N., Burrows D., Osborne J. P., 2007a, ApJ, 663, 505

Ness J. et al., 2007b, ApJ, 665, 1334

Ness J. et al., 2003, ApJL, 594, L127

Ness J., Starrfield S., Jordan C., Krautter J., Schmitt J. H. M. M., 2005, MNRAS, 364, 1015

O'Brien T. J., Lloyd H. M., Bode M. F., 1994, MNRAS, 271, 155

Ögelman H., Krautter J., Beuermann K., 1987, A&A, 177, 110

Orio M. et al., 2003, IAUcirc, 8131, 2

Osborne J. et al., 2006a, The Astronomer's Telegram, 764, 1

Osborne J. et al., 2006b, The Astronomer's Telegram, 801, 1

Osborne J. et al., 2006c, The Astronomer's Telegram, 770, 1

Osborne J. P. et al., 2011, ApJ, 727, 124

Osborne J. P. et al., 2010, The Astronomer's Telegram, 2442, 1

Page K. L., Osborne J. P., Beardmore A. P., Goad M. R., Wynn G. A., Bode M. F., O'Brien T. J., 2008, in Evans A., eds, ASP Conf. Series, Vol. 401, p. 283

Page K. L. et al., 2010, MNRAS, 401, 121

Petz A., Hauschildt P. H., Ness J.-U., Starrfield S., 2005, A&A, 431, 321

Pinto C., Ness J.-U., Verbunt F., Kaastra J. S., Costantini E., Detmers R. G., 2012, A&A, 543, A134

Rauch T., Orio M., Gonzales-Riestra R., Nelson T., Still M., Werner K., Wilms J., 2010, ApJ, 717, 363

Rohrbach J. G., Ness J., Starrfield S., 2009, AJ, 137, 4627

Roming P. W. A. et al., 2005, Space Sci. Rev., 120, 95

Schaefer B. E., 1990, ApJL, 355, L39

Schaefer B. E., 2005, ApJL, 621, L53

Schaefer B. E. et al., 2010, AJ, 140, 925

Schlegel E. M. et al., 2010, The Astronomer's Telegram, 2419, 1

Schwarz G. J. et al., 2011, ApJS, 197, 31

Shore S. N. et al., 2003, AJ, 125, 1507

Starrfield S., Iliadis C., Hix W. R., 2008, in Bode M., Evans A., eds, Classical Novae, Cambridge University Press, p. 77

Strüder L. et al., 2001, A&A, 365, L18

Turner M. J. L. et al., 2001, A&A, 365, L27

van Rossum D., 2009, Ph.D. Thesis, University of Hamburg

van Rossum D., Ness J., 2010, AN, 331, 175

van Rossum D. R., 2012, ArXiv e-prints

Vaytet N. M. H., O'Brien T. J., Page K. L., Bode M. F., Lloyd M., Beardmore A. P., 2011, ApJ, 740, 5